

Original Research

Low dose Streptozotocin Induced Organopathies in Normoglycemic Rabbits

¹Masood Saleem Mir, ²Reashma Roshan, ³Omer Khalil Baba, ⁴Aarif Ali, ⁵Showkeen Muzamil Bashir

^{1,3}Division of Veterinary Pathology Faculty of Veterinary Sciences & Animal Husbandry, SKUAST-Kashmir, Alusteng, Shuhama, J&K, India;

²Department of Hematology, Sher-i-Kashmir Institute of Medical Sciences (SKIMS), Soura Srinagar, J&K, India;

^{4,5}Division of Veterinary Biochemistry, Faculty of Veterinary Sciences & Animal Husbandry, SKUAST-Kashmir, Alusteng, Shuhama, J&K, India

ABSTRACT:

Purpose: Present investigation was aimed at characterization of pathomorphological lesions in the low doses streptozotocin intoxicated normoglycemic rabbits. **Method:** Streptozotocin was administered (@65mg/kg b.w, as single intravenous dose followed by glucose therapy after 9 hours in New Zealand White rabbits having 1-1.5 kg body weight. . Blood glucose was regularly monitored and animals reverting to normoglycemic state on day 7 following STZ administration were used for study. Two rabbits each were sacrificed fortnightly from days 15 to 60 for pathoanatomical investigation. **Results:** Gross pathological alterations included congestion and varying degree of haemorrhages in different organs; and oedema and softness of pancreas. Histopathologically, pancreatic islets of Langerhans were variably affected ranging from normal through degranulation, degeneration, loss of beta cells to complete cell loss. Regenerative changes were evident at later stages. Liver revealed vascular congestion, progressive hepatosis, portal hepatitis, Kupffer cell hyperplasia, binucleated hepatocytes, and at later stage cholangitis, portal fibrosis and necrosis. Kidneys showed vascular congestion, focal haemorrhages; tubular nephrosis; lower nephron nephrosis; glomerular congestion, hypersegmentation and atrophy; mesangial cell hyperplasia; and occasionally, peritubular fibroplasia and casts in collecting tubules. At later stages vacuolation of podocytes with glomerular degeneration and mononuclear cell infiltration were seen with focal nephritis. Neuronal degeneration was observed in brain along with necrosis in cerebral cortex, hippocampus including dentate gyrus, cornu Ammonis especially CA4 region, subiculum, caudoputamen, and cerebellum; oedema, demyelination, and neuronophagic nodule in cerebrum; congestion of choroid plexus and periependymal inflammation; and Purkinje cell degeneration in cerebellum. Lungs revealed vascular congestion, haemorrhage, emphysema, atelectasis, oedema, denudation of bronchial and bronchiolar epithelium, peribronchial lymphoid hyperplasia, focal to diffuse mononuclear cell infiltration, bronchitis, bronchial epithelial hyperplasia and focal interstitial pneumonia. Heart revealed haemorrhages; degeneration and necrosis of cardiomyocytes; Purkinje cell degeneration and mononuclear cell infiltration. Spleen and MLNs revealed congestion, haemorrhage, apoptosis of lymphoid cells, and histiocyte vacuolation. Adrenal gland revealed congestion, haemorrhage, oedema, degenerative changes in zona fasciculata and mononuclear cell infiltration. Changes in testes were characteristic of arrested spermatogenesis, and degeneration and apoptosis of spermatocytes. **Conclusion:** The pathological changes observed in streptozotocin treated rabbits reflect its potential toxic effects in other organs at least in rabbits.

Received: 19 November, 2021

Accepted: 22 December, 2021

Corresponding author: Masood Saleem Mir, Division of Veterinary Pathology Faculty of Veterinary Sciences & Animal Husbandry, SKUAST-Kashmir, Alusteng, Shuhama, J&K, India

This article may be cited as: Mir MS, Roshan R, Baba OK, Ali A, Bashir SM. Low dose Streptozotocin Induced Organopathies in Normoglycemic Rabbits. J Adv Med Dent Scie Res 2022;10(1):128-142.

INTRODUCTION

Streptozotocin (STZ), an *N*-methyl-*N*-nitrosoureido D-glucosamine derivative, is frequently used in development of rodent diabetic models for screening the compounds including natural products for their insulinomimetic, insulinotropic and other

hypoglycaemic/ antihyperglycaemic activities (Lei *et al.*, 2005; Sharma *et al.*, 2006; Patel *et al.*, 2006; Lenzen, 2008). Insulin producing β cells are selectively destroyed by it, whereas, other pancreatic alpha and delta cells are left intact (Szkudelski, 2001). This is attributed to its selective uptake and

accumulation in pancreatic β -cells via the low-affinity GLUT2 glucose transporter selectively expressed in pancreatic islets (Elsner *et al.*, 2000). Both T1DM and T2DM has been induced by STZ which is preferred over other diabetogenic drugs because of its more specific action, wider safe dose, relatively longer half-life (15 min), production of sustained hyperglycemia for longer duration and development of well characterized diabetic complications with fewer incidences of ketosis and less mortality (Srinivasan and Ramarao, 2007). Species, strain, sex and nutritional state plays important role in the variation of sensitivity and there are batch differences in activity (Okamoto, 1981; Honjo *et al.*, 1986; Kramer *et al.*, 2009). While cat and human pancreatic β -cells have been reported to be resistant to the diabetogenic action of STZ (Hatchell *et al.*, 1986; Yang and Wright, 2002), guinea pigs and marmoset are less sensitive (Losert *et al.*, 1971; Kramer *et al.*, 2009). Rabbits given low dose of STZ, although showed typical betacytolysis associated early hypoglycemia followed by hyperglycemia, failed to develop sustained hyperglycemia and reverted to normoglycemia within 7 days (Mir *et al.*, 2015; 2016). Diabetogenic action of STZ has been prevented by reduced expression of GLUT2 the (Schnedl *et al.*, 1994; Thulesen *et al.*, 1997) and GLUT2 expression *in vivo* and *in vitro* is itself restricted when STZ is administered in multiple doses. (Wang and Gleichmann, 1995; 1998).

The pathological alterations observed in STZ models have been essentially attributed to hyperglycemia as the cells not expressing the GLUT2 receptors are resistant (Elsner *et al.*, 2000; Arkkila *et al.*, 2001; Zafar *et al.*, 2009b). Also, STZ is less lipophilic and rather highly hydrophilic preventing its free entry into the cells as well as access to the brain via the blood-brain barrier (Schnedl *et al.*, 1994; Ran *et al.*, 2007). However, toxic effects have been reported in organs with certain level of GLUT2 glucose transporter, particularly kidney and liver (Rerup, 1970; Weiss, 1982; Thorens *et al.*, 1988; Piyachaturawat *et al.*, 1988 & 1990). In the present study investigation of STZ induced pathomorphological effects in normoglycemic STZ treated rabbits was done.

MATERIALS AND METHODS

EXPERIMENTAL ANIMALS

New Zealand white rabbits were procured from Laboratory Animal Resource and maintained under standard conditions in cage system. Study was conducted on rabbits with three months age and weighing about 1-1.5 kg. The Institutional Animal Ethics Committee approved the experimental protocols involved in this study. Before the start of the experiments, all the animals were acclimatized for a period of 7 days. Equal random allocation was followed for constitution of experimental groups.

Feed and water was given *ad libitum* to the rabbits whereas, rabbit feed and greens were given twice a day (morning and evening).

DEVELOPMENT OF EXPERIMENTAL MODEL

Rabbits were fed in the morning and then fasted for 18 hours providing only water during the period. The blood glucose level of fasting period was determined using glucometer (Accu-Chek, Roche diagnostics India Pvt. Ltd., Mumbai). The beta-cytotoxic drug streptozotocin (Sigma-Aldrich) was given as slow intravenous injection @65mg/kg body weight in 1ml freshly prepared citrate buffer, pH 4.6 through ear vein using insulin syringe. Freshly prepared solutions of the calculated dose of drugs were used. After administration of beta-cytotoxic drugs rabbits were examined for immediate effects vis-à-vis changes in blood glucose levels, and clinical signs. Rabbits were given 5ml of 25% dextrose intraperitoneally at 9 hours post alloxan administration, and 10% glucose in drinking water up to 24 hours post-treatment, followed by normal management. Fasting blood glucose levels were recorded at days 3, 5 and 7 following administration of streptozotocin. Animals reverting to normoglycemic state on day 7 following STZ administration were used for study.

PATHOANATOMICAL STUDIES

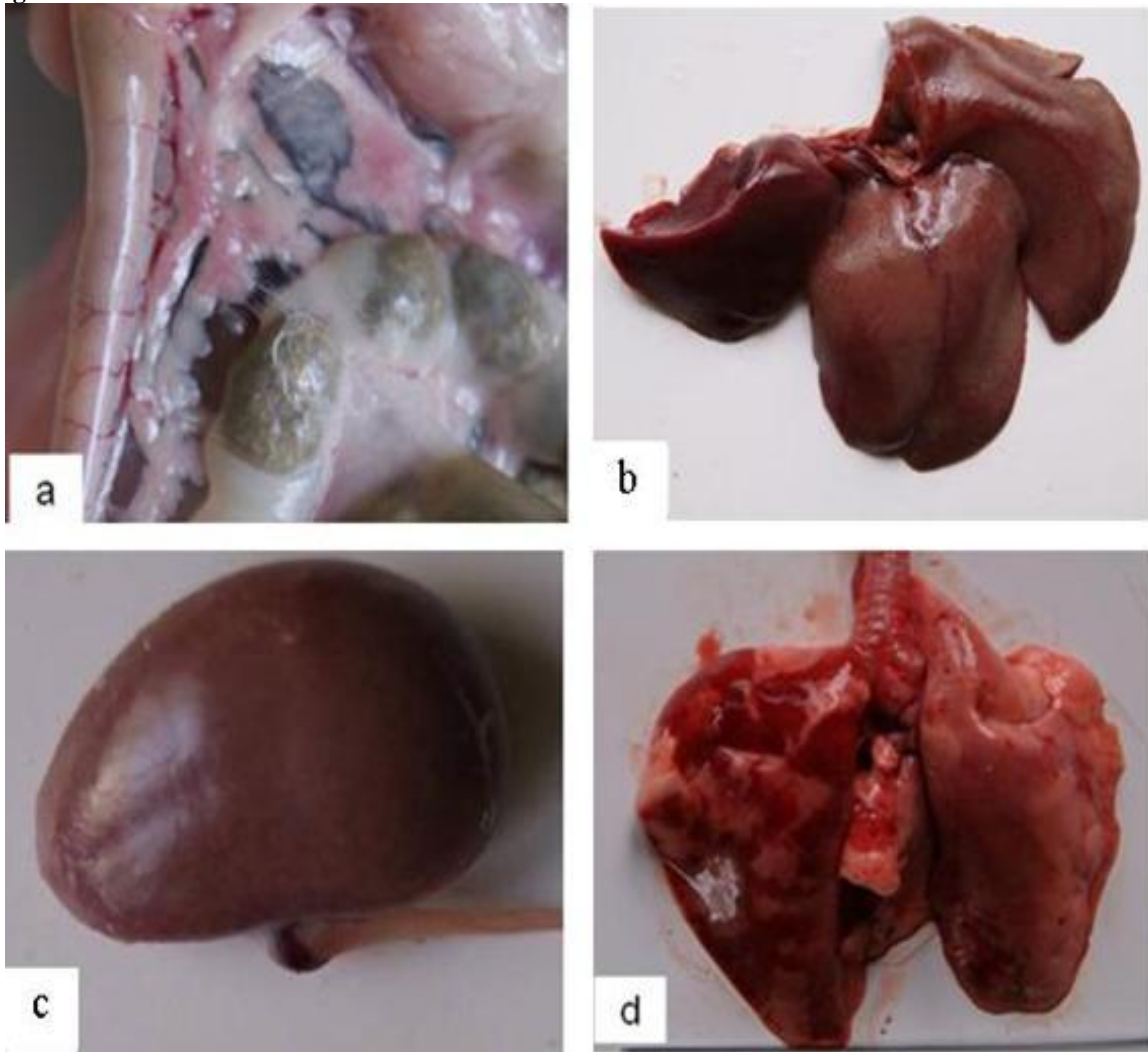
For pathoanatomical investigations two rabbits each from STZ treated and control group were euthanized on day 15, 30, 45, and 60. Gross lesions were noted following complete systematic necropsy examination by Rokitansky's method. For histopathology, representative tissue samples from all the organs were collected and 10% formol saline was used for their preservation. Processing for paraffin embedding was done by using alcohol as dehydrating agent and benzene as clearing agent. The sections were cut at 4-5 μ m thickness and stained by Harris' haematoxylin and eosin method. Alcian-Blue PAS (AB-PAS) was used as a special stain for acid and neutral mucopolysaccharides (Luna, 1968)

RESULTS

GROSS PATHOLOGY

The rabbit sacrificed during the period of study revealed pale/ anemic mucous membranes. Pancreas initially appeared soft, oedematous and congested. Congestion was not evident during later period. Liver revealed congestion, petechiae and ecchymotic haemorrhages. Kidneys showed congestion, petechiae and mottling. Both cortical and medullary congestion was present. Lungs revealed emphysema, congestion and haemorrhage with the predominance of the former in the right lung while left revealed suffusions and areas of red hepatization (Fig. 1).

Fig. 1: Streptozotocin treated rabbits: a) Pancreas at day15 appearing soft, oedematous and congested; b) Liver at day 60 revealing petechiae and areas of suffusions, c) Kidney at day 60 revealing congestion and petechiae. d) Lungs at day 30 showing areas of red hepatisation in left lung and emphysematous right lung.



HISTOPATHOLOGY PANCREAS

At day 15 pancreatic islets were variedly affected. While some islets appeared normal, most of them revealed varying degrees of hypocellularity with beta cell loss. The surviving beta-cells revealed degeneration and degranulation (Fig. 2a). Complete loss of the cells was indicated by observing only cellular debris giving it a ghost islet appearance. Acinar cells by large appeared normal, otherwise degenerative and lytic changes were occasionally noted. Congestion occurred both in the interlobular septa and parenchyma.

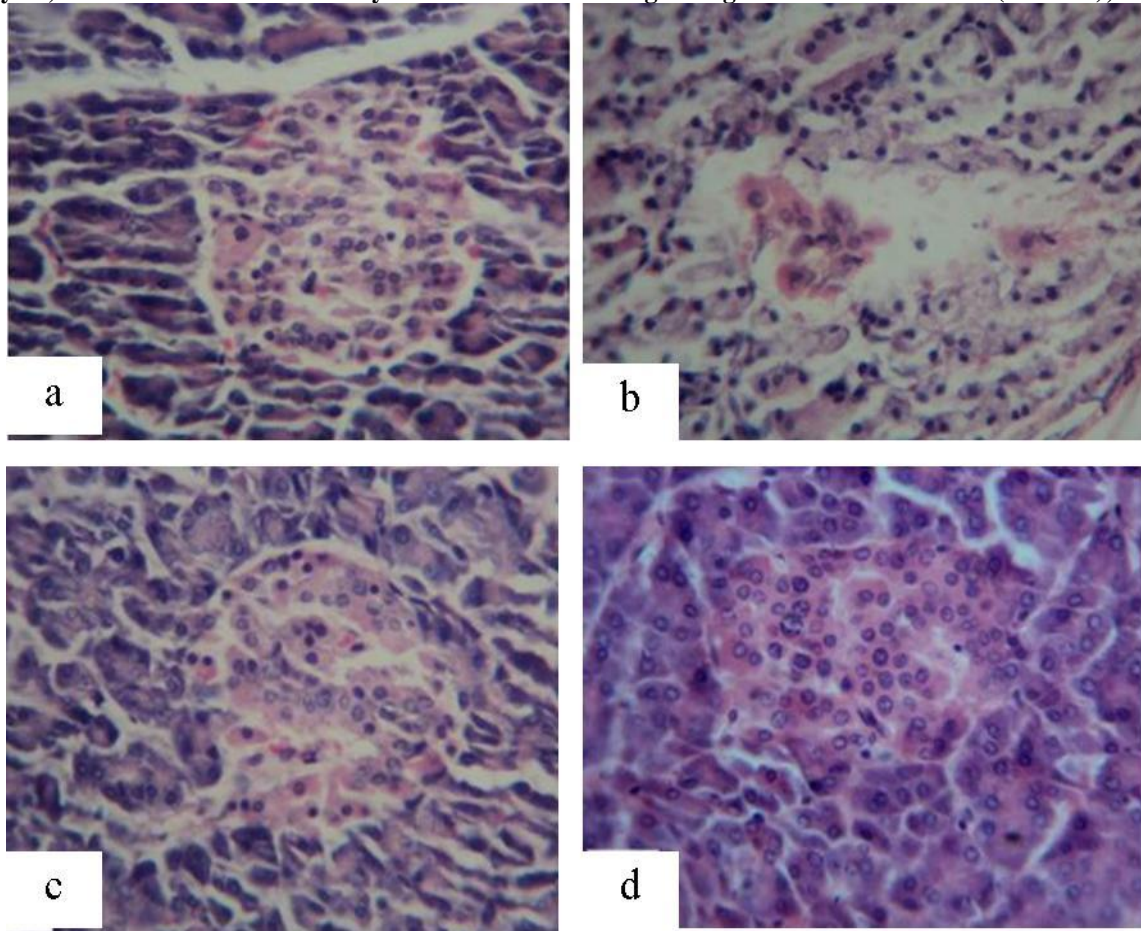
At day 30, most of the islets revealed moderate to severe hypocellularity with partial to complete beta-cell loss (Fig. 2b). A number of ghost islets were observed. Only a few islets were either normal or revealed degenerating or degranulating beta-cells. Distorted acini revealed marked cellular degeneration

characterized by cellular swelling, vacuolation and condensation of nuclei. Pancreatic acini were more severely affected around the severely affected islets. Marked vascular congestion was noted in interlobular septa.

At day 45, the islets were largely hypocellular and the cells were spindle shaped revealing hyperchromatic nuclei. Occasionally, islet cells were in form of chords (Fig. 2c) or revealed beta cell lysis. Vascular congestion was marked. Acinar cells mostly appeared normal.

At day 60, islets were mostly normal. Occasionally, islets revealed cellular degranulation, lysis and hypocellularity of mild to moderate nature (Fig. 2d). Hypocellular islets showed presence of spindle cells with nuclear hyperchromatism. Moderate vascular congestion, and normal acinar cells were present.

Fig. 2: Section of pancreas a) day 15, revealing, Islet with beta cells undergoing degenerative and lytic changes. H.E. x400 (OZ x4.0); b) day 30, Markedly hypocellular islet. Note the presence of only few cells. H.E. x400 (OZ x4.0); c) day 45, Hypocellular islet with presence of cells in chords H.E. x400 (OZ x4.0); d) day 60, Islet with normal cellularity and beta cells revealing mild granulation. H.E. x400 (OZ x4.0);



LIVER

At day 15 the most prominent change was hepatocellular degeneration characterized by cellular swelling with rounding of borders and rarefaction of cytoplasm giving it a vacuolar appearance. The changes were more severe in periportal regions. Binucleated hepatocytes were frequently observed (Fig. 3a). Occurrence of scattered or focal collections of mononuclear cell infiltration accompanied with Kupffer cell hyperplasia was a consistent finding. Comparatively more prominent infiltrations were in periportal regions. Cholangitis with mononuclear cell infiltration was observed. Biliary hyperplasia associated with mild to severe necrosis and denudation was seen. Additionally, liver showed mild to moderate vascular congestion.

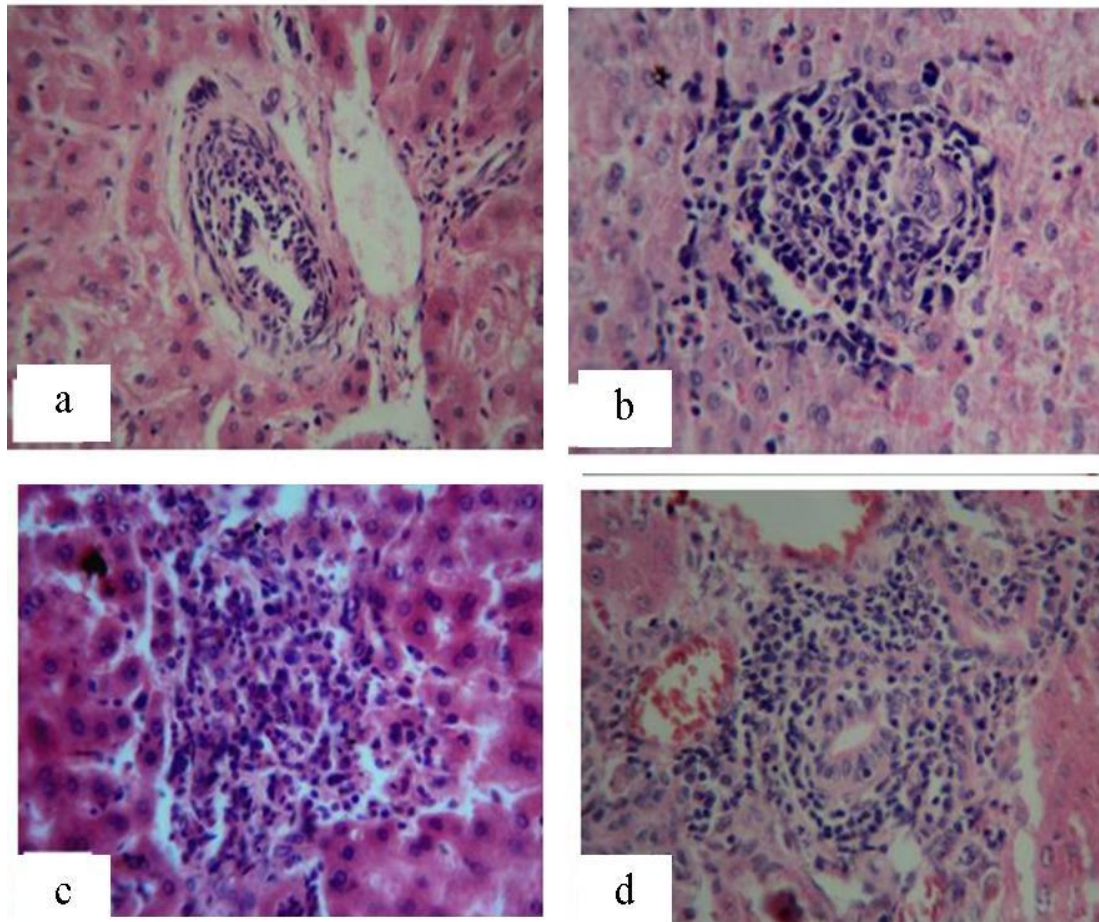
At day 30 hepatocellular degeneration characterized by cellular swelling with rounding of cells and vacuolar changes continued along with mild to moderate congestion. Focal hepatitis was denoted by infiltration of admixture of mononuclear cells and

epithelioid cells associated with localized hepatocellular necrosis (Fig. 3b). Portal triaditis and cholangitis was a prominent feature paralleled with mild to severe necrosis and denudation of lining epithelium of bile ductules and duct.

At day 45 varying degrees of hepatocellular degeneration frequently lead to distortion of hepatic chords. Focal hepatitis, portal triaditis and cholangitis were observed. Binucleated hepatocytes with granular eosinophilic cytoplasm were numerous seen in the adjacent area (Fig. 3c). Vascular congestion and haemorrhage continued.

At the day 60 hepatocellular degeneration was denoted by granular cytoplasm with increased eosinophilia, and cellular swelling causing compression of sinusoids. Vacuolar changes were shown by hepatocytes in subcapsular region. Focal hepatitis, portal triaditis and cholangitis with mononuclear cell infiltration were prominently observed (Fig. 3d).

Fig. 3: Section of liver a) day 15, Hepatocellular degeneration, binucleated hepatocytes, and mononuclear cell infiltration in biliary ductule. H.E. x400 (OZ x2.8); b) day 30, Focal hepatitis with hepatocellular necrosis and mononuclear cell infiltration. Note the presence of epithelioid cells. H.E. x400 (OZ x4.0); c) day 45, Focal hepatitis. H.E. x400 (OZ x4.0); d) day 60, Portal triaditis . H.E. x400 (OZ x3.5).



KIDNEYS

At day15 kidneys revealed diffuse vascular congestion and varying degrees of cortical nephrotic changes. Focal haemorrhages were evident which were prominent in cortico-medullary junction. Disintegration of the basement membrane caused tubular distortions. Glomeruli revealed congestion, hypersegmentation and mesangial cell hyperplasia (Fig. 4a). Atrophy of glomeruli was occasionally observed. Peritubular fibroplasia was observed. Medulla revealed lower nephron nephrosis, vascular congestion and focal haemorrhages. Tubular cell degeneration was characterized by increased cytoplasmic eosinophilia and granularity, and nuclear rarefaction. Cytolysis, karyorrhexis and karyolysis were evident in more severely affected tubules. Detached lining epithelium was observed in some tubular lumens.

At day 30 marked tubular degeneration and necrosis, along with breaks in the basement membranes, were observed in PCTs and DCTs. Peritubular fibroplasia was present at a few places. Glomeruli revealed congestion and hypersegmentation. Mesangial cell hyperplasia and vacuolar changes in the podocytes were evident (Fig. 4b). The changes were prominent

at the cortico-medullary junction denoted by tubular nephrosis, vascular congestion and haemorrhages. Similar changes were revealed in renal medulla. Frequently, rupture of the tubular basement membrane was noted. Collecting tubules, also, revealed vacuolar changes in the lining epithelium and epithelial casts were present in the lumens.

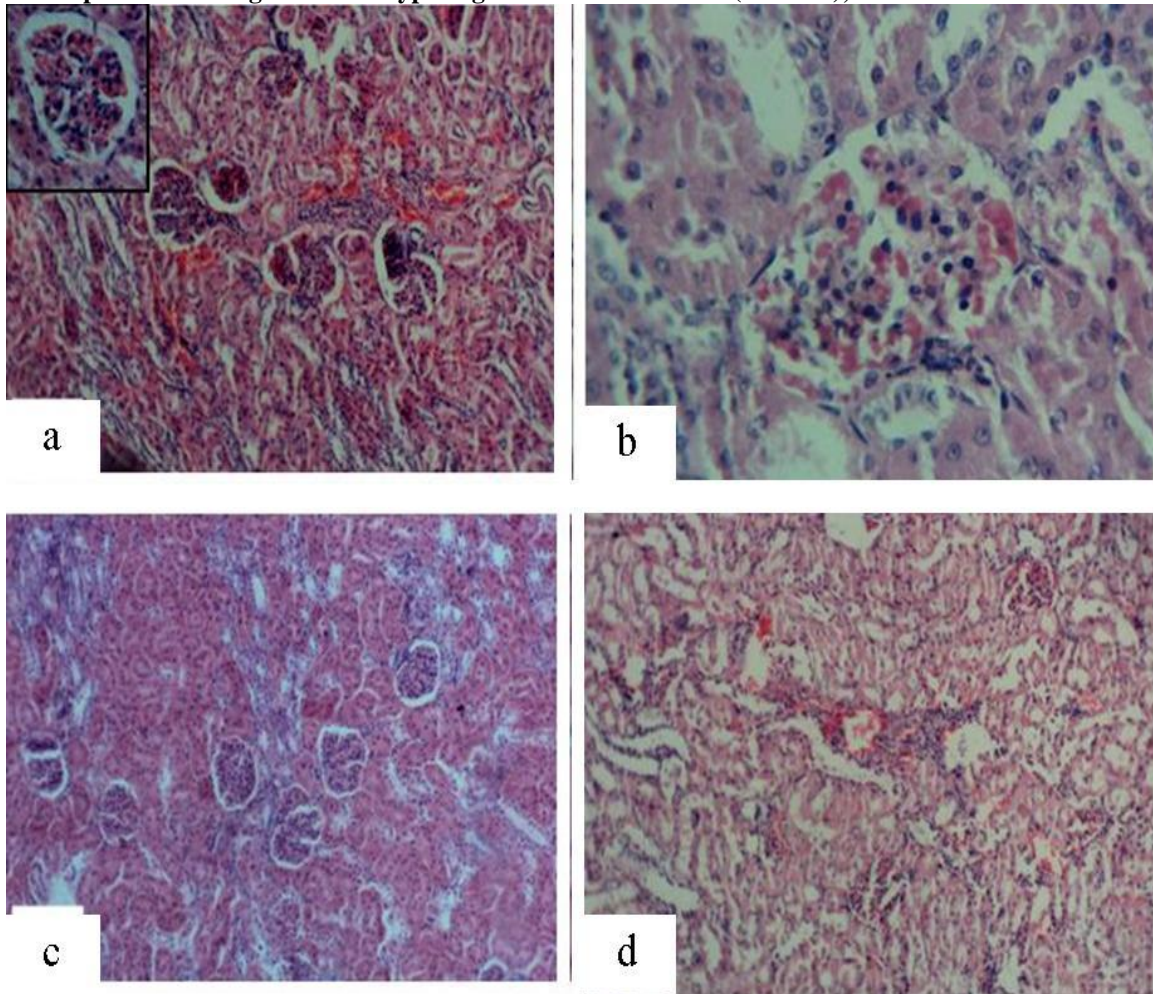
At day 45 renal cortex revealed degeneration of PCTs and DCTs characterized by cellular swelling.. Peritubular fibroplasia was occasionally seen. Glomeruli revealed hypersegmentation, vacuolar changes in the podocytes and increased number of mesangial cells (Fig. 4c). Renal medulla revealed lower nephron nephrosis. Detachment of tubular epithelium from the basement membrane was a frequent observation. Degenerating epithelium was characterized by large rarefied nuclei. However, some cells had pyknotic and hyperchromatic nuclei.

At day 60 severe degeneration, lysis and denudation of cortical tubular epithelium were frequently seen along with breaks in basement membrane (Fig. 4d). Glomeruli revealed congestion, hypersegmentation and fragmentation. At places loss of tubular architecture with areas of necrosis, infiltration of mononuclear cells and haemorrhages were observed.

Focal nephritis characterized by mononuclear cell infiltration associated with severe vascular congestion and haemorrhages were prominent in cortico-medullary region. Renal medulla revealed lower

nephron nephrosis, haemorrhages and mononuclear cell infiltration. Collecting tubules revealed vacuolar changes, haemorrhages, and granular casts in the lumens. Chronic nephritis was also observed.

Fig. 4: Section of kidney a) day 15, Focal haemorrhage, glomerular congestion and hypersegmentation, and tubular nephrosis. H.E. x100 (OZ x4.0) ; Insert: Higher magnification showing glomerular congestion and hypersegmentation. H.E. x400 (OZ x4.0); b) degeneration of tubular lining epithelium and glomerular congestion. H.E. x400 (OZ x4.0); c) day 45, glomerular hypersegmentation with vacuolar changes in podocytes and mesangial cell hyperplasia. H.E. x100 (OZ x4.0); d) day 60, Degeneration of tubular epithelium and glomerular hypersegmentation. H.E. x100 (OZ x4.0);



BRAIN

At day 15, cerebral cortex revealed degeneration and necrosis of pyramidal and granule cells with increased cytoplasmic basophilia (Fig. 5a). Satellitosis and neuronophagia were observed. The latter had occasionally resulted in formation of clear spaces. Oedema, mild to moderate gliosis and demyelination were noted. Hippocampus showed neuronal degeneration and necrosis. Dentate gyrus showed neuronal degeneration characterized by dissolution of nissl granules and nuclear rarefaction. Neurons occasionally showed increased cytoplasmic eosinophilia and nuclear basophilia (Fig. 5b). All the regions of *Cornu Ammonis* revealed similar changes. Degeneration and necrosis was more extensive in pyramidal cells of CA4 region. Extensive

degeneration of neurons and necrosis with satellitosis and neuronophagia were observed in subiculum. Meningeal and cerebral vessels revealed congestion. Cerebellum revealed focal degeneration and necrosis of purkinje cells.

At day 30 changes were similar but comparatively more severe than at day15. Widespread degeneration and necrosis of granule and pyramidal neurons with satellitosis and neuronophagia were observed in cerebral cortex (Fig. 5c) including caudoputamen. Mild neuronal degeneration and necrosis in dentate gyrus was observed in hippocampus, *Cornu Ammonis* especially CA4 region and subiculum. Meningeal congestion was marked. Choroid plexus revealed congestion and inflammation was noted in periependymal region (Fig. 5d). Neuronal

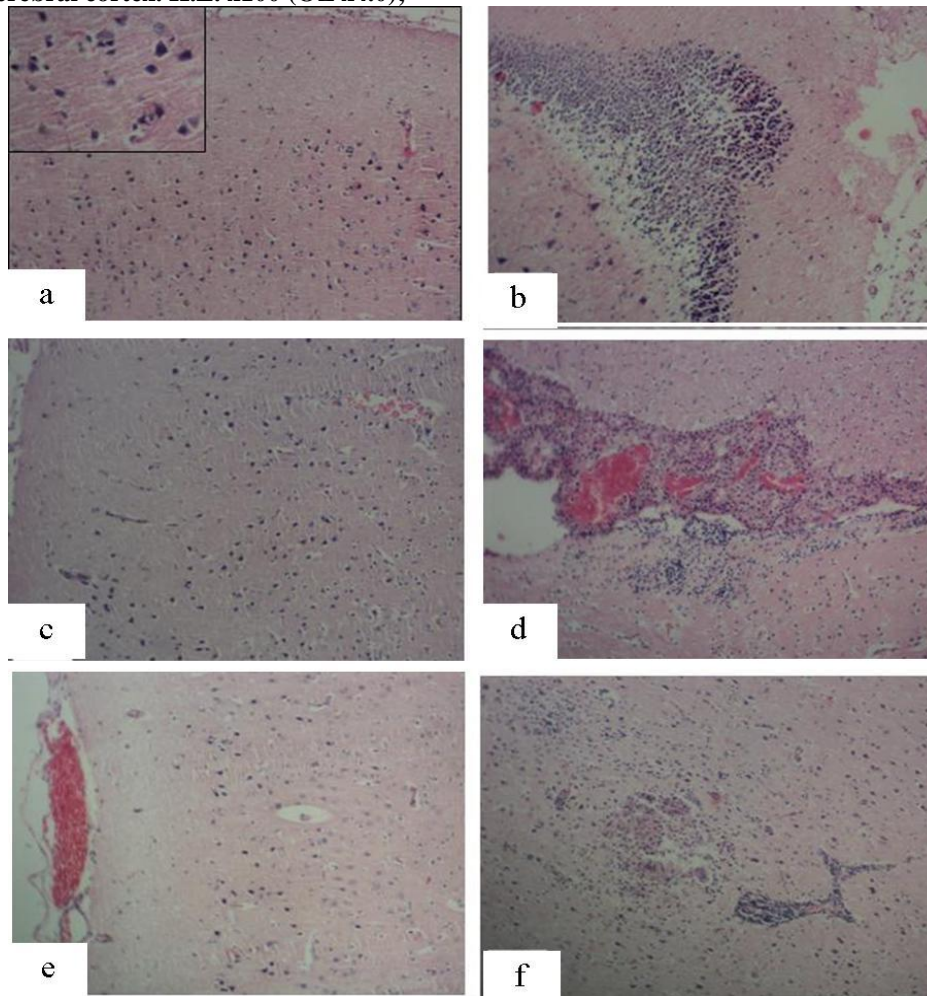
degeneration, necrosis, satellitosis, neuronophagia and demyelination were prominent in brain stem. Cerebellum appeared normal except for presence of focal degeneration of purkinje cells.

At day 45, degenerative changes and granular necrosis and pyramidal neurons with satellitosis and neuronophagia were observed in different areas of the cerebral cortex including caudoputamen (Fig. 5e). Also, demyelination was noted. Neuronal degeneration, with loss of nissl substance and rarefaction of nuclear chromatin material associated with satellitosis and neuronophagia, were also observed in dentate gyrus and different areas of *Cornu Ammonis*. CA4 was more severely affected Subiculum revealed compressed microvasculature with clear perivascular space, neuronal degeneration and necrosis. Congestion of meningeal vessels and choroid plexus was noted. Only focal degeneration

and necrosis were observed in purkinje cells in cerebellum.

At day 60, Microvascular congestion and focal haemorrhages were noted in the cerebrum. Neuronal degeneration was observed in cerebral cortex and necrosis with chromatolysis, satellitosis and neuronophagia. Gliosis and demyelination were observed in different areas of cortex. Focal necrotic areas, formation of neuronophagic nodule and marked perivascular cuffing were occasionally noted (Fig. 5f). Degeneration of the neurons, necrosis and demyelination were observed in caudatoputamen, different regions of hippocampus including dentate gyrus *Cornu Ammonis* and subiculum; and brain stem. Widespread congestion of meningeal vessels was seen. Cerebellum revealed microvascular congestion, and focal degeneration and necrosis of purkinje cells.

Fig. 5: Section of brain a) day 15, Degeneration of pyramidal cells. H.E. x100 (OZ 4.0) ; Insert: Higher magnification. H.E. x400 (OZ x4.0); b) day 15, Necrosis of neurons in dentate gyrus. H.E. x100 (OZ x4.0) ; c) day 30, Neuronal degeneration and necrosis in cortex. Note condensed neurons. H.E. x100 (OZ x4.0); d) day 30, Congestion of choroid plexus and peri-ependymal inflammation. H.E. x100 (OZ x4.0); e) day 45, Congestion of meningeal vessels and degeneration of neurons in the cerebral cortex. H.E. x400 (OZ x4.0); f) day 60, Perivascular cuffing, gliosis and necrosis of neurons with formation of neuronophagic nodule in cerebral cortex. H.E. x100 (OZ x4.0);



LUNG

At day 15 lungs revealed vascular congestion and haemorrhages. Haemorrhages were severe in subpleural area. Alveolar oedema, emphysema, and atelectasis in the adjacent areas were the prominent lesions. Focal to diffuse mononuclear cell infiltrations were evident. Bronchi and bronchioles showed denudation of lining epithelium. Peribronchial lymphoid hyperplasia was occasionally observed (Fig. 6a).

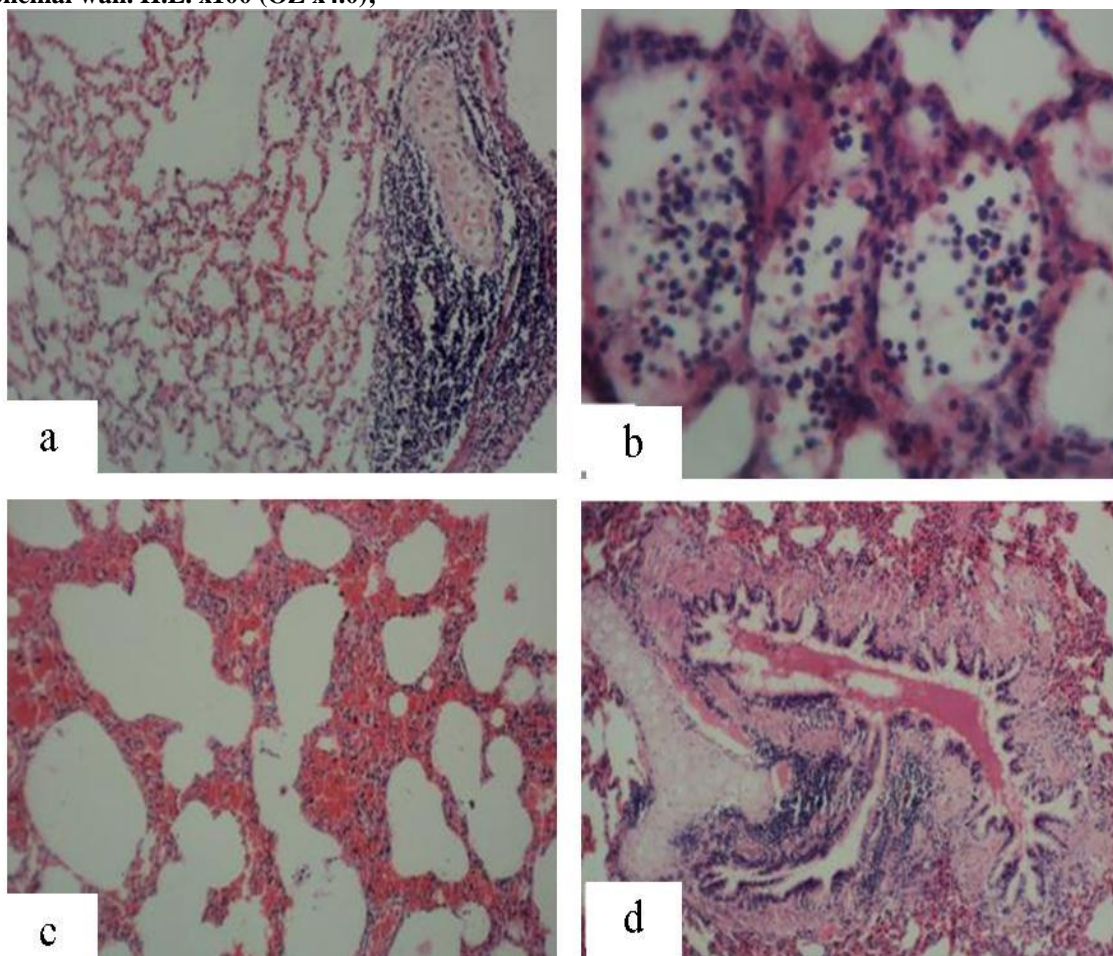
At day 30, severe congestion and variable degrees of haemorrhages were observed in alveoli and bronchioles. Marked emphysema and atelectasis were

seen. Haemorrhagic debris was seen in the bronchial lumens. Bronchitis associated with peribronchial lymphoid hyperplasia was a frequent observation. Lymphocyte and macrophage infiltration was noted in the alveoli (Fig. 6b).

At day 45, changes were similar characterized by congestion, haemorrhage, emphysema and focal interstitial lymphocytic infiltration (Fig. 6c).

At day 60, marked haemorrhages were seen. Emphysema and oedema were consistently observed. Focal interstitial pneumonia and bronchitis were noted. Bronchi revealed epithelial hyperplasia (Fig. 6d).

Fig. 6: Section of lung a) day 15, Vascular congestion, alveolar emphysema and peri-bronchial lymphoid hyperplasia. H.E. x100 (OZ x4.0); b) day 30, Presence of alveolar macrophages. H.E. x400 (OZ x4.0). c) day 45, Haemorrhage and atelectasis. H.E. x100 (OZ x3.0) ; d) day 60, Infiltration of mononuclear cells in bronchial wall. H.E. x100 (OZ x4.0);

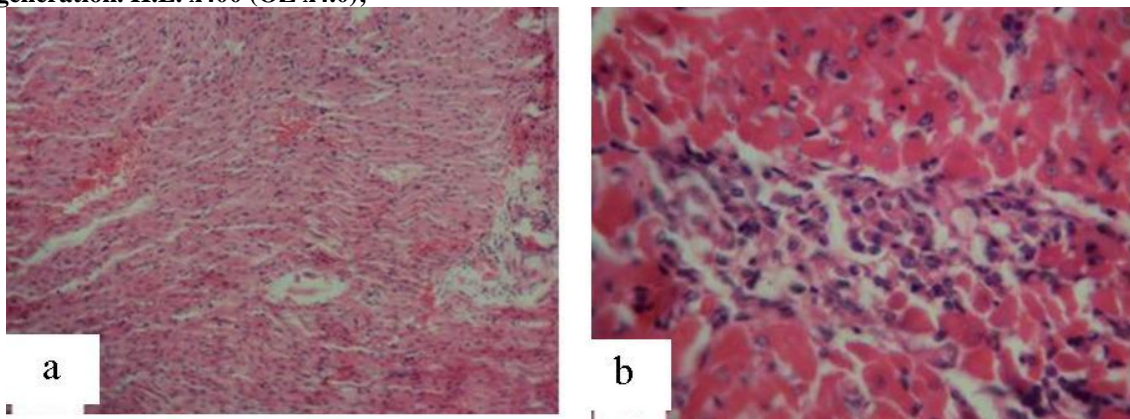


HEART

The changes in the heart appeared at day 30 and comprised of focal areas of haemorrhages in myocardium (Fig. 7a) cusps of atrio-ventricular valves, and degeneration and necrosis of cardiomyocytes. Changes were similar at day 45 and by day 60 cardiomyocytes showed degeneration with

increased cytoplasmic eosinophilia, nuclear pyknosis and nuclear rarefaction. Vacuolar changes were noted in epicardial myocytes. Degenerative change was, also, observed in pericardium. Purkinje cell degeneration was intermittently observed (Fig. 7b). Mononuclear cell infiltration was observed throughout the myocardium.

Fig. 7: Section of heart a) day 15, Haemorrhages. H.E. x100 (OZ x4.0) ; b) day 60, Purkinje cell degeneration. H.E. x400 (OZ x4.0);



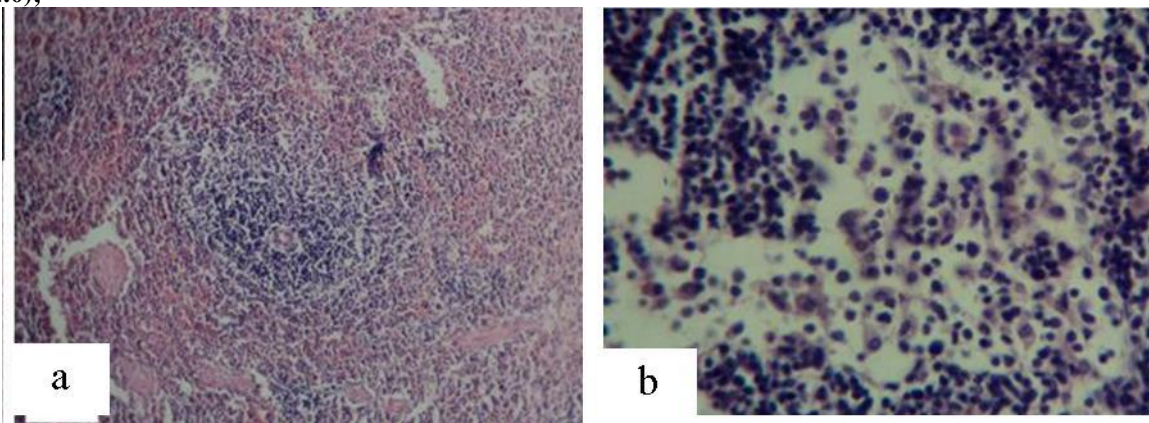
SPLEEN

At day 15, spleen revealed congestion of sinusoids, mild haemorrhage and rarefaction in white pulp. Changes akin to apoptosis were seen in lymphoid cells. Vacuolation was observed in histocytes (Fig. 8a). At day 30 post-treatment lymphoid cell depletion and apoptosis were more severe along with marked vacuolation of histocytes. The changes at day 45 and day 60 did not reveal any marked variation.

MESENTERIC LYMPH NODE

MLN, at day 15, revealed vascular congestion and focal haemorrhage. Varying degrees of lymphoid cell depletion were noted in follicles. Severely affected follicles revealed apoptosis of lymphoid cells associated with histiocytic reaction in paracortex and medullary area. Changes were similar but more prominent at day 30 (Fig. 8b). Lymphoid depletion, at days 45 and 60, was comparatively more severe causing rarefaction of the cortex. Thinning of the mantle zone and medullary cords was prominent.

Fig. 8: Section a) spleen, day 15 Loss of lymphoid cells in white pulp. H.E. x100 (OZ x4.0). ; b) Mesenteric Lymphnode, day 15, Depletion of lymphoid cells and reactive histiocytosis. H.E. x400 (OZ x4.0);



ADRENAL GLAND

At days 15 and 30, adrenal revealed slight congestion especially in cortico-medullary junction area. Cells in zona fasciculate showed degenerative changes. At day 45 and 60, all layers of cortex and medulla showed vascular congestion. Haemorrhages and oedema were observed in deeper cortex and medulla. Cells in zona fasciculate showed vacuolation. Mononuclear cell infiltration was sparsely evident.

Spermatogonial cells frequently appeared in multiple layers. Multinucleated spermatids were occasionally seen. At day 30 and 45, number of spermatogonial cells had decreased and degenerative changes were observed. At day 60, the spermatocytes revealed vacuolation and apoptotic changes.

TESTES

At day 15, testes revealed vascular congestion. Seminiferous tubules showed spermatogonia and primary spermatocytes in the pachytene stage.

DISCUSSION

Grossly congestion and varying degree of haemorrhages were evidenced in different organs reflecting the toxic effects of STZ. The oedema and softness of pancreas may be attributed to predominant beta-cytotoxic nature of the drug. Histopathologically, pancreatic islets of Langerhans were variably affected.

During early periods, while most of the islets revealed marked loss of β -cells and some even complete cell loss, appreciable number of islets were either normal or showed only degranulation or partial β -cell loss. These changes were in concordance with earlier workers (Mir *et al.*, 2008b). The STZ induced beta-cytolysis has been described in earlier section. The persistence of islets with partial or complete cell loss indicates irreversible damage leading to necrosis and apoptosis (Liu *et al.*, 2000; Szkudelski, 2001; Liu *et al.*, 2004; Slawson *et al.*, 2005; Pathak *et al.*, 2008). Variable susceptibility of individual cells within a single islet as well as of different islets has been reported (Mir *et al.*, 2008b). Aybar *et al.* (2001) have reported that use of lower dose of STZ produced an incomplete destruction of pancreatic β -cells even though rats became permanently diabetic. In present study, quick recovery from hyperglycemic state and maintenance of normoglycemia for prolonged period may be attributed to presence of normal islets. Appearance of degranulating and degenerating β -cells till late during the experiment probably indicates the metabolic stress warranting hyper-secretion from the functional islets (Arora *et al.*, 2009). This may, however, also, be a normal physiological process. It is generally accepted that β -cells have a finite life span and that dying β -cells are continuously replaced (Finegood *et al.*, 1995; Pick *et al.*, 1998; Montanya, 2000; Dor *et al.*, 2004; Bonner-Weir *et al.*, 2004;). Appearance of spindle cells with nuclear hyperchromatism, during later stage, indicated of regenerative process. The regenerative process may be favoured by the maintenance of normoglycemia. It has been observed that the glycemic control by insulin therapy favours β -cell regeneration in STZ induced diabetic models (Grossman 2010). Degeneration of acinar cells observed at early stage reflects direct action of heavy release of insulin (Meral *et al.*, 2001). Derangements in cellular Ca^{2+} and Mg^{2+} homeostasis has been associated with STZ induced exocrine inefficiency (Patel *et al.*, 2004 & 2006).

Liver revealed vascular congestion, progressive hepatosis, portal hepatitis, Kupffer cell hyperplasia and presence of binucleated hepatocytes. During later stage cholangitis associated with portal fibrosis and necrosis were seen. The changes correlated well with progressive alteration of ALT and AST. Similar changes have been reported by other workers following STZ treatment (Das *et al.*, 1996; Degirmenchi *et al.*, 2002; Mir *et al.*, 2008b; Zafar *et al.*, 2009b; Nahla and Refat, 2012). However, in all these studies STZ treatment had produced hyperglycemia and glucotoxicity was considered predominant factor. The normoglycemic conditions suggest direct hepatotoxic effects of STZ. Alternatively, the hyperlipidaemia might have played some role in hepatotoxicity (Ohno *et al.*, 2000; Merzouk *et al.*, 2000). The vacuolar change observed in the hepatocytes may be attributed to glycogen depletion (Das *et al.* 1996; Thulesen *et al.*, 1997;

Zafar *et al.*, 2009b). While progressive change depicts an irreversible damage, the presence of binucleated hepatocytes indicated concurrent regenerative process. The inflammatory reaction predominated in portal area. Zafar *et al.* (2009b) reported varying degree of inflammatory infiltrate in the portal tract which caused destruction of the smaller (interlobular and septal) intrahepatic bile ducts and also, biliary hyperplasia in some cases.

Kidneys revealed vascular congestion, focal haemorrhages, cortical tubular degeneration with disintegration of basement membrane, and lower nephron nephrosis. Changes in glomeruli ranged from congestion, hypersegmentation and mesangial cell hyperplasia to atrophy. Occasionally, peritubular fibroplasia and casts in collecting tubules were observed. At later stages glomerular degeneration with vacuolation of podocytes, focal tubular necrosis, and focal nephritis with mononuclear cell infiltration were seen. At places chronic nephritis was evident. The progressive pathoanatomical alterations are in agreement with the observed alterations in KFT. Varying degree of nephropathy has been reported by different workers (Honjo *et al.*, 1986; Bansal *et al.*, 1994; Sandhu *et al.*, 2000). Zafar *et al.* (2009a) reported progressive damage which increased with the duration of time. While most of the workers have attributed the nephropathic effects to STZ induced hyperglycemia (Rasch, 1984; Kramer *et al.*, 2009), STZ induced-delayed type of renal toxicity has also been suggested (Rakieten *et al.*, 1968; Okawa and Doi, 1983). Also, single large dose of STZ has been observed to cause direct acute renal damage in the proximal tubular epithelium in mice (Levine *et al.*, 1980). Contrary to this, Scott *et al.* (1989) reported that diabetogenic dose of STZ (55 mg/kg, ip) was not toxic to kidneys. They observed that BUN and renal cortical slice uptake of p-aminohippurate (PAH) and tetraethylammonium (TEA) were not altered, relative to normoglycemic rats, 3, 16, and 28 days following STZ treatment. Mir *et al.* (2008b) reported only renal congestion in STZ-diabetic rabbits. Kidneys receiving high blood supply and being the main excretory organs for STZ (Sicor Pharmaceuticals, 2003) are an important target organ for a prolonged period. Expression of high level of GLUT-2 receptors favour rapid uptake of STZ by kidneys. In present study, although hyperglycemia was not observed, the progressive hyperlipidaemia indicates metabolic disturbance. Excessive production and accumulation of lipids has been associated with alteration in renal structure and function (Yotsumoto *et al.*, 1997). The nephritic lesions and peritubular fibrosis may be attributed to STZ induced oxidative stress leading to hypoxia as is evidenced by the disintegration of basement membrane. The oxidative stress associated with hypoxia and tubular epithelial damage may be incriminated for setting up of the proinflammatory response resulting in nephritis and peritubular fibroplasias (Tang *et al.*, 2003; Hirschberg and Wang,

2005; Ruster and Wolf, 2008; Magri and Fava, 2009; Vallon, 2011)

Wide spread pathoanatomical alterations were noted in brain involving cerebral cortex, hippocampus including dentate gyrus, *cornu Ammonis* especially CA4 region, subiculum, caudoputamen, and cerebellum. Cerebrum revealed neuronal degeneration and necrosis, associated with satellitosis, neuronophagia, gliosis, oedema and demyelination. Cerebellum showed focal Purkinje cell degeneration. Changes were progressively severe. At later stages congestion of choroid plexus and periependymal inflammation was noted. At day 60 focal necrotic areas with formation of neuronophagic nodule and marked perivascular cuffing were noted. Diabetic doses of STZ have been reported to cause marked changes in energy metabolism of brain involving almost all regions (Mans *et al.*, 1988). Intracerebroventricular application of low doses of STZ in rats have been found to cause severe disturbances in insulin system involving down regulation of the expression of insulin-1 and -2 mRNA, and Insulin receptor (IR) mRNA in hippocampus and frontoparietal cerebral cortex; increased protein tyrosine kinase activity in hippocampus; decreased total IR β -subunit in hypothalamus; and increase in phosphorylated IR tyrosine residues leading to generation of hyperphosphorylated tau protein which plays important role as a morphological marker of sporadic Alzheimer's disease. Also STZ has been found to induce disturbance in learning and memory capacities (Grünblatt *et al.*, 2007; Plaschke *et al.*, 2010). Contrary to our histopathological observations, Plaschke *et al.* (2010) did not observe any necrotic or apoptotic change. However, Lester-Coll *et al.* (2006) reported marked pathomorphological alterations including reduced brain size and degeneration of neurons with cell loss, gliosis, and increased immunoreactivity for p53, active glycogen synthase kinase 3 β , phospho-tau, ubiquitin, and amyloid- β , following intracerebral administration of STZ in rats. Various authors have ascribed STZ induced encephalopathy and neuropathy to hyperglycemia induced oxidative stress resulting in lipid peroxidation (Arnal *et al.*, 2010; Shanmugam *et al.*, 2011; Alp *et al.*, 2012; Uzar *et al.*, 2012). In present study, STZ induced brain damage was not associated with hyperglycemia. However, STZ is known to cause redox disturbances directly (Nukatsuka *et al.*, 1990a; Turk *et al.*, 1993). Also role of some subtle metabolic disturbances, as evidenced by hyperlipidaemia, cannot be ruled out.

Lungs revealed vascular congestion, haemorrhage, emphysema and atelectasis, oedema, denudation of bronchial and bronchiolar epithelium, peribronchial lymphoid hyperplasia, and focal to diffuse mononuclear cell infiltration. At later stages bronchitis, bronchial epithelial hyperplasia and focal interstitial pneumonia was noted. STZ induced

diabetes has been found to cause pulmonary functional abnormalities, such as a reduction in elastic recoil, lung volumes, and pulmonary diffusing capacity, reduced forced vital capacity and forced expiratory volume in one second (Sahebajami and Denholm, 1988). Thickening of the alveolar basement membranes with increase in the relative amounts of collagen, elastin, and basal laminae in the alveolar wall and more alveoli per unit volume has been observed in STZ-induced diabetic rats (Kida *et al.*, 1983). Pulmonary venous resistance has been found to be selectively increased 2 weeks after the induction of STZ diabetes (Russ and Tobin, 1996). Congestion, haemorrhage and oedema may be attributed to changes in the capillary and venular epithelium (Popov and Simionescu, 1997).

Heart revealed haemorrhages, and degeneration and necrosis of cardiomyocytes. At advanced stages Purkinje cell degeneration and mononuclear cell infiltration was observed which could not be attributed to glucotoxicity as reported by previous workers (Mir *et al.*, 2008b). Muruganandan *et al.* (2002) observed that myocardial haemorrhage and hypertrophy were associated with significantly increased cardiac superoxide dismutase (SOD), catalase (CAT) and lipid peroxidation.

Spleen and mesenteric lymph nodes revealed congestion, haemorrhage, apoptosis of lymphoid cells, and histiocyte vacuolation. This is in agreement with the observed leukocytopenia. The direct immunosuppressant effects of STZ has been reported by previous workers (Nichols *et al.*, 1981; Handwerker 1984).

Adrenal gland revealed congestion, haemorrhage, oedema, degenerative changes in zona fasciculata and mononuclear cell infiltration. The alterations reflect stress associated changes. Increased hypothalamo-pituitary-adrenal activity has been associated with STZ induced diabetes (Chan *et al.*, 2001). Morphological and microvascular changes in the adrenal gland of diabetic rats were reported by Sricharoenvej *et al.* (2009)

Changes in testes were characteristic of arrested spermatogenesis, and degeneration and apoptosis of spermatocytes. Although, direct toxicity of STZ to testes has not been reported, structural and functional alterations have been observed in STZ-induced diabetic models. Disruption of spermatogenesis (maturation arrest) along with altered structure has been observed by Hassan and Moneim (2001).

Present study revealed that single intravenous dose of STZ caused progressive functional and morphological alterations without development of hyperglycemia. The changes are suggestive of direct toxicity and/or oxidative damage besides subtle metabolic disturbances. The pathomorphological alterations in pancreas suggest that rabbits are not totally refractive to beta-cytolysis. It seems that higher doses may be required for development of diabetes, which however may not serve as a good model in view of the

observed toxic effects of sub-diabetogenic dose and regeneration of β -cells. In present study, only fasting glucose levels were considered and rabbits were not evaluated for postprandial glucose tolerance. Low dose of Alloxan has been reported to induce glucose intolerance among rabbits (Puri, 2006). The author reported initial fasting hyperglycemia followed by returning of the fasting blood glucose to normal or near normal levels. However, the blood glucose levels were higher following oral glucose load in the 1, 2, and 3h samples, reflecting glucose intolerance. The nature and severity of STZ-induced diabetes has been found to vary with respect to dose, route of drug, and species of animal. It has been used to develop both T1DM and T2DM with hypoinsulinaemia. Mild to severe diabetes has been reported following i.v. or i.p. administration of the drug (Arora *et al.*, 2009; Etuk, 2010).

CONCLUSION

The pathological changes observed in streptozotocin treated rabbits reflect its potential toxic effects in other organs at least in rabbits.

REFERENCES

- Alp, H., Varol, S., Celik, M.M., Altas, M., Evliyaoglu, O., Tokgoz, O., Tanrıverdi, M.H. and Uzar, E. 2012. Protective effects of beta glucan and gliclazide on brain tissue and sciatic nerve of diabetic rats induced by streptozosin. *Experimental Diabetes Research* **2012**:230342.
- Arkkila, P.E., Koskinen, P.J., Kantola, I.M., Ronnema, T., Seppanen, E. and Viikari, J.S. 2001. Diabetic complications are associated with liver enzyme activities in people with type-1 diabetes. *Diabetes Research and Clinical Practice* **52(2)**:113-118.
- Arnal, E., Miranda, M., Barcia, J., Bosch-Morell, F. and Romero, F.J. 2010. Lutein and docosahexaenoic acid prevent cortex lipid peroxidation in streptozotocin-induced diabetic rat cerebral cortex. *Neuroscience* **166(1)**:271-278.
- Arora, S., Ojha, S.K. and Vohora, D. 2009. Characterisation of streptozotocin induced diabetes mellitus in swiss albino mice. *Global Journal of Pharmacology* **3 (2)**:81-84.
- Aybar, M.J., Sanchez Riera An., Grau, A. and Sanchez, S.S. 2001. Low dose of STZ produced an incomplete destruction of pancreatic β -cells in rats. *Journal of Ethnopharmacology* **27**: 243-247.
- Bansal, B.K., Mohan, R., Bansal, N., Pawar, H.S. and Nauriyal, D.C. 1994. Alloxan diabetes in dogs: clinical and pathoanatomical observations. *Indian Journal of Veterinary Pathology* **18(2)**: 138-141.
- Bonner-Weir, S., Toschi, E., Inada, A., Reitz, P., Fonseca, S.Y., Aye, T. and Sharma, A. 2004. The pancreatic ductal epithelium serves as a potential pool of progenitor cells. *Pediatric Diabetes* **5(Suppl)**:216-222.
- Chan, O., Chan, S., Inouye, K., Vranic, M. and Matthews, S.G. 2001. Molecular regulation of the hypothalamo-pituitary-adrenal axis in streptozotocin-induced diabetes: effects of insulin treatment. *Endocrinology* **142**:4872-4879.
- Das, A.V., Padayatti, P.S. and Paulose, C.S. 1996. Effect of leaf extract of *Aegle marmelose* (L.) Correa ex Roxb. On histological and ultrastructural changes in tissues of Streptozotocin induced diabetic rats. *Indian Journal of Experimental Biology* **34(4)**:341-345.
- Degirmenchi, I., Kalender, S., Ustuner, M.C., Kalender, Y., Gunes, H.V., Unal, N. and Basaran, A. 2002. The effects of acarbose and *Rumex patientia* on liver ultrastructure in streptozotocin-induced diabetic (type-II) rats. *Drugs under Experimental and Clinical Research* **28**:229-34.
- Dor, Y., Brown, J., Martinez, O.I. and Melton, D.A. 2004. Adult pancreatic β cells are formed by self-duplication rather than stem cell differentiation. *Nature* **429**:41-46.
- Elsner, M., Guldbakke, B., Tiedge, M., Munday, R. and Lenzen, S. 2000. Relative importance of transport and alkylation for pancreatic beta-cell toxicity of streptozotocin. *Diabetologia* **43**:1528-1533.
- Etuk, E.U. 2010. Animal models for studying diabetes mellitus. *Agriculture and Biology Journal of North America* **1(2)**:130-134.
- Finegood, D.T., Scaglia, L. and Bonner-Weir, S. 1995. Dynamics of beta-cell mass in the growing rat pancreas. Estimation with a simple mathematical model. *Diabetes* **44**:249-256.
- Grossman, E.J., Lee, D.D., Tao, J., Wilson, R.A., Park, S.Y., Bell, G.I. and Chong, A.S. 2010. Glycemic control promotes pancreatic beta-cell regeneration in streptozotocin-induced diabetic mice. *PLoS ONE* **5(1)**:e8749.
- Grünblatt, E., Salkovic-Petrisic, M., Osmanovic, J., Riederer, P. and Hoyer, S. 2007. Brain insulin system dysfunction in streptozotocin intracerebroventricularly treated rats generates hyperphosphorylated tau protein. *Journal of Neurochemistry* **101(3)**:757-70.
- Handwerker, B.S., Fernandes, G., Riehm, T., Sutherland, D.E. and Brown, D.M. 1984. Alterations in immunological function in streptozotocin-induced murine diabetes mellitus: correction by islet cell transplantation. *Clinical Immunology and Immunopathology* **32(3)**: 275-284.
- Hassan, G.M.A. and Moneium, T.A. 2001. Structural changes in the testes of streptozotocin-induced diabetic rats. *Suez Canal University Medical Journal* **4(1)**:17-25.
- Hatchell, D.L., Reiser, H.J., Bresnahan, J.F. and Withworth, U.G. 1986. Resistence of cats to the diabetogenic effect of alloxan. *Laboratory Animal Science* **36**:37-41.
- Hirschberg, R. and Wang, S. 2005. Proteinuria and growth factors in the development of tubulointerstitial injury and scarring in kidney disease. *Current Opinion in Nephrology and Hypertension* **14**:43-52.
- Honjo, K., Doi, K., Doi, C. and Mitsuoka, T. 1986. Histopathology of streptozotocin-induced diabetic DBA/2N and CD-1 mice. *Laboratory animals* **20**:298-303.
- Kida, K., Utsuyama, M., Takizawa, T. and Thurlbeck, W.M. 1983. Changes in lung morphologic features and elasticity caused by streptozotocin-induced diabetes mellitus in growing rats. *American Review of Respiratory Disease* **128**:125-131.
- Kramer, J., Moeller, E.L., Hachey, A., Mansfield, K.G. and Wachtman, L.M. 2009. Differential expression of GLUT2 in pancreatic islets and kidneys of New and Old World nonhuman primates. *American Journal of*

- Physiology- Regulatory. Integrative and Comparative Physiology* **296(3)**: R786–R793.
24. Lei, Y.C., Hwang, J.S., Chan, C.C., Lee, C.T. and Cheng, T.J. 2005. Enhanced oxidative stress and endothelial dysfunction in streptozotocin-diabetic rats exposed to fine particles. *Environmental Research* **99**:335–343.
 25. Lenzen, S. 2008. The mechanisms of alloxan- and streptozotocin-induced diabetes. *Diabetologia* **51**:216–226.
 26. Lester-Coll, N., Rivera, E.J., Soscia, S.J., Doiron, K., Wands, J.R. and de la Monte, S.M. 2006. Intracerebral streptozotocin model of type 3 diabetes: relevance to sporadic Alzheimer's disease. *Journal of Alzheimers Disease* **9(1)**:13–33.
 27. Levine, B.S., Henry, M.C., Port, C.D. and Rosen, E. 1980. Toxicologic evaluation of streptozotocin (NSC85998) in mice, dogs and monkeys. *Drug and Chemical Toxicology* **3**:201–212.
 28. Liu, J.P., Zhang, M., Wang, W.Y. and Grimsgaard, S. 2004. Chinese herbal medicines for type-2 diabetes mellitus. *Cochrane Database of Systematic Reviews* **3**:3642.
 29. Liu, K., Paterson, A.J., Chin, E. and Kudlow, J.E. 2000. Glucose stimulates protein modification by O-linked GlcNAc in pancreatic β cells: linkage of O-linked GlcNAc to β cell death. *Proceedings of National Academy of Science USA* **97**:2820–2825.
 30. Losert, W., Rilke, A., Loge, O. and Richter, K.D. 1971. Vergleichende biochemische untersuchungen uber die diabetogene wirkung von streptozotocin bei mausen, ratten, chinesischen streifen-hamstern und meerschweinchen. *Arzneim Forsch* **21**:1643–1653.
 31. Luna L.G., 1968. *Manual of Histologic Staining Methods of the Armed Forces Institute of Pathology*, (3rd Edn.), McGraw-Hill Book Company, New York.
 32. Magri, C.J. and Fava, S. 2009. The role of tubular injury in diabetic nephropathy. *European Journal of Internal Medicine* **20**: 551–555.
 33. Mans, A.M., DeJoseph, M.R., Davis, D.W. and Hawkins, R.A. 1988. Brain energy metabolism in streptozotocin-diabetes. *Biochemical Journal* **249**:57–62.
 34. Meral, I., Yener, Z., Kahraman, T. and Mert, N. 2001. Effect of *Nigella sativa* on glucose concentration, lipid peroxidation, anti-oxidant defence system and liver damage in experimentally-induced diabetic rabbits. *Journal of veterinary medicine. A, physiology, pathology, clinical medicine* **48**:593–599.
 35. Merzouk, H., Madani, S., Chabane, S. D., Prost, J., Bouchenak, M. and Belleville, J. 2000. Time course of changes in serum glucose, insulin, lipids and tissue lipase activities in macrosomic offspring of rats with Streptozotocin induced diabetes. *Clinical Science* **98(1)**:21–30.
 36. Mir, M.S., Darzi, M.M., Baba, O.K., Khan, H.M., Kamil, S.A., Sofi, A.H. and Wani, S.A. 2015. Streptozotocin Induced Acute Clinical Effects in rabbits (*Oryctolagus cuniculus*). *Iranian Journal of Pathology*, **10(3)**: 206–213
 37. Mir, M.S., Darzi, M.M., Baba, O.K., Shah, A.A., Qureshi, S. and Khan, H.M., 2016. Comparative evaluation of diabetogenic potentials of alloxan, streptozotocin and their cocktail in rabbits (*Oryctolagus cuniculus*). *Applied Biological Research*, **18**: 61–65; DOI: 10.5958/0974-4517.2016.00009.4
 38. Mir, S.H., Baqui, A., Bhagat, R.C., Darzi, M.M. and Shah, A.W. 2008. Biochemical and histomorphological study of streptozotocin-induced diabetes mellitus in rabbits. *Pakistan Journal of Nutrition* **7(2)**:359–364.
 39. Montanya, E., Nacher, V., Biarnes, M. and Soler, J. 2000. Linear correlation between beta-cell mass and body weight throughout the lifespan in Lewis rats: role of beta-cell hyperplasia and hypertrophy. *Diabetes* **49**:341–346.
 40. Muruganandan, S., Gupta, S., Kataria, M., Lal, J. and Gupta, P.K. 2002. Mangiferin protects the streptozotocin-induced oxidative damage to cardiac and renal tissues in rats. *Toxicology* **176(3)**:165–173.
 41. Nahla, A.G. and Refat, A. 2012. Efficacy of *N. sativa* oil and Glimepiride on the histopathological changes of streptozotocin-induced diabetic rats. *Journal of American Science* **8(3)**:22–33.
 42. Nichols, W.K., Vann, L.L and Spellman, J.B. 1981. Streptozotocin effects on T lymphocytes and bone marrow cells. *Clinical and Experimental Immunology* **46(3)**:627–632.
 43. Nukatsuka, M., Yoshimura, Y., Nishida, M. and Kawada, J. 1990a. Allopurinol protects pancreatic beta cells from the cytotoxic effect of streptozotocin: in vitro study. *Journal of Pharmacobiodynamics* **13**:259–262.
 44. Ohno, T., Horio, F., Tanaka, S., Terada, M., Namikawa, T. and Kitch, J. (2000). Fatty liver and hyperlipidemia in IDDM (insulin dependent diabetes mellitus) of Streptozotocin treated shrews. *Life Science* **66(2)**:125–131.
 45. Okamoto, H. 1981. Regulation of proinsulin synthesis in pancreatic islets and a new aspect to insulin dependent diabetes. *Molecular and Cellular Biochemistry* **37**:43–61.
 46. Okawa, H. and Doi, K. 1983. Neoplastic lesions in streptozotocin-treated rats. *Experimental Animals (Tokyo)* **32**:77–84.
 47. Patel, R., Shervington, A., Pariente, J.A., Martinez-Burgos, M.A., Salido, G.M., Adeghate, E. and Singh, J. 2006. Mechanism of exocrine pancreatic insufficiency in streptozotocin-induced type 1 diabetes mellitus. *Annals of the New York Academy of Sciences* **1084**:71–88.
 48. Patel, R., Yago, M.D., Mañas, M., Victoria, E.M., Shervington, A. and Singh, J. 2004. Mechanism of exocrine pancreatic insufficiency in streptozotocin-induced diabetes mellitus in rat: effect of cholecystokinin-octapeptide. *Molecular and Cellular Biochemistry* **261(1-2)**:83–89.
 49. Pathak, S., Dorfmüller, H.C., Borodkin, V.S. and van Aalten, D.M.F. 2008. Chemical dissection of the link between streptozotocin, O-GlcNAc, and pancreatic cell death. *Chemical Biology* **15(8)**:799–807.
 50. Pick, A., Clark, J., Kubstrup, C., Levisetti, M., Pugh, W., Bonner-Weir, S. and Polonsky, K.S. 1998. Role of apoptosis in failure of beta-cell mass compensation for insulin resistance and beta-cell defects in the male Zucker diabetic fatty rat. *Diabetes* **47**:358–364.
 51. Piyachaturawat, P., Poprasit, J. and Glinsukon, T. 1990. Gastric mucosal secretions and lesions by different doses of Streptozotocin in rats. *Toxicology Letters* **55**:21–29.
 52. Piyachaturawat, P., Poprasit, J., Glinsukon, T. and Warichanon, C. 1988. Gastric mucosal lesions in Streptozotocin diabetic rats. *Cell Biology International Reports* **12(1)**:53–63.
 53. Plaschke, K., Kopitz, J., Siegelin, M., Schliebs, R.,

- Salkovic-Petrisic, M., Riederer, P. and Hoyer, S. 2010. Insulin-resistant brain state after intracerebroventricular streptozotocin injection exacerbates Alzheimer-like changes in Tg2576 AbetaPP-overexpressing mice. *Journal of Alzheimer's Disease* **19(2)**:691-704.
54. Popov, D. and Simionescu, M. 1997. Alterations of lung structure in experimental diabetes, and diabetes associated with hyperlipidaemia in hamsters. *European Respiratory Journal*, **10**:1850–1858.
 55. Puri, D. 2006. Screening mildly hypoglycaemic compounds: Obese British angora rabbits with borderline glucose intolerance as animal model. *Scientific Publication of the Indian Pharmacological Association* **68(5)**:579-583.
 56. Rakieten, N., Gordon, B.S., Cooney, D.A., Davis, R.D. and Schein, P.S. 1968. Renal tumorigenic action of streptozotocin (NSC85998) in rats. *Cancer Therapy Reports* **52**:563-567.
 57. Ran, C., Pantazopoulos, P., Medarova, Z. and Moore, A. 2007. Synthesis and testing of β -cell-specific streptozotocin-derived near-infrared imaging probes *Angewandte Chemie-International Edition In English* **46**:8998–9001.
 58. Rasch, R. 1984. Tubular lesions in streptozotocin diabetic rats. *Diabetologia* **27**:32-37.
 59. Rerup, C.C. 1970. Drugs producing diabetes through damage of the insulin secreting cells. *Pharmacological Reviews* **22 (4)**:485-518.
 60. Russ, R.D. and Tobin, B.W. 1996. Alteration of segmental vascular resistance in the pulmonary circulation of diabetic rats. *Canadian Journal of Physiology Pharmacology* **74**:1010–1015.
 61. Ruster, C. and Wolf, G. 2008. The role of chemokines and chemokine receptors in diabetic nephropathy. *Frontiers in Bioscience* **13**:944–955.
 62. Sahebajami, H. and Denholm, D. 1988. Effects of streptozotocin-induced diabetes on lung mechanics and biochemistry in rats. *Journal of Applied Physiology* **64(1)**:147-153.
 63. Sandhu, K., Randhawa, S.S. and Brar, R.S. 2000. Clinical and pathological changes in alloxan induced diabetes mellitus alone and in combination with ethylene glycol induced nephropathy in dogs. *Indian Journal of Veterinary Pathology* **24**:12–15.
 64. Schnedl, W.J., Ferber, S., Johnson, J.H. and Newgard, C.B. 1994. STZ transport and cytotoxicity. Specific enhancement in GLUT2- expressing cells. *Diabetes* **43**:1326–1333.
 65. Schnedl, W.J., Ferber, S., Johnson, J.H. and Newgard, C.B. 1994. STZ transport and cytotoxicity. Specific enhancement in GLUT2- expressing cells. *Diabetes* **43**:1326–1333.
 66. Scott, L.A., Madan, E. and Valentovic, M.A. 1989. Attenuation of cisplatin nephrotoxicity by streptozotocin-induced diabetes. *Fundamental and Applied Toxicology* **12(3)**:530-539.
 67. Shanmugam, K.R., Mallikarjuna, K., Kesireddy, N. and Sathyavelu Reddy, K. 2011. Neuroprotective effect of ginger on anti-oxidant enzymes in streptozotocin-induced diabetic rats. *Food and Chemical Toxicology* **49(4)**:893–897.
 68. Sharma, S.B., Nasir, A., Prabhu, K.M., Murthy, P.S. 2006. Antihyperglycemic effect of the fruit-pulp of *Eugenia jambolana* in experimental diabetes mellitus. *Journal of Ethnopharmacology* **104**:367–373.
 69. Sior Pharmaceuticals. 2003. Material Safety Data Sheet. Sior Pharmaceuticals Inc. Irvine CA.
 70. Slawson, C., Zachara, N.E., Vosseller, K., Cheung, W.D., Lane, M.D. and Hart, G.W. 2005. Perturbations in O-linked β -N-acetylglucosamine protein modification cause severe defects in mitotic progression and cytokinesis. *Journal of Biological Chemistry* **280**:32944–32956.
 71. Sricharoenvej, S., Boonprasop, S., Lanlua, P., Piyawinijwong, S. and Niyomchan, A. 2009. Morphological and microvascular changes of the adrenal glands in streptozotocin-induced long-term diabetic rats. *Italian Journal of Anatomy and Embryology* **114(1)**:1-10.
 72. Srinivasan, K. and Ramarao, P. 2007. Animal models in type 2 diabetes research: An overview. *Indian Journal of Medical Research* **125**:451-472.
 73. Srinivasan, K. and Ramarao, P. 2007. Animal models in type 2 diabetes research: An overview. *Indian Journal of Medical Research* **125**:451-472.
 74. Szkudelski, T. 2001. The mechanism of alloxan and streptozotocin action in β -cells of the rat pancreas. *Physiological Research* **50**:536-546.
 75. Tang, S., Leung, J.C., Abe, K., Chan, K.W., Chan, L.Y., Chan, T.M. and Lai, K.N. 2003. Albumin stimulates interleukin-8 expression in proximal tubular epithelial cells in vitro and in vivo. *The Journal of Clinical Investigation* **111**:515–527.
 76. Thorens, B., Sarkar, H.K., Kaback, H.R. and Lodish, H.F. 1988. Cloning and functional expression in bacteria of a novel glucose transporter present in liver, intestine, kidney, and beta-pancreatic islet cells. *Cell* **55**:281-290.
 77. Thulesen, J., Orskov, C., Holst, J.J. and Poulsen, S.S. 1997. Short term insulin treatment prevents the diabetogenic action of streptozotocin in rats. *Endocrinology* **138(1)**:62-68.
 78. Turk, J., Corbett, J.A., Ramanadham, S., Bohrer, A. and McDaniel, M.L. 1993. Biochemical evidence for nitric oxide formation from streptozotocin in isolated pancreatic islets. *Biochemical and Biophysical Research Communications* **197**:1458–1464
 79. Uzar, E., Alp, H., Cevik, M.U., Firat, U., Evliyaoglu, O., Tufek, A. and Altun, Y. 2012. Ellagic acid attenuates oxidative stress on brain and sciatic nerve and improves histopathology of brain in streptozotocin-induced diabetic rats. *Neurological Sciences* **33(3)**:567-74.
 80. Vallon, V. 2011. The proximal tubule in the pathophysiology of the diabetic kidney. *American Journal of Physiology - Regulatory, Integrative and Comparative Physiology* **300**:R1009–R1022.
 81. Wang, Z. and Gleichmann, H. 1995. Glucose transporter 2 expression: prevention of streptozotocin-induced reduction in beta-cells with 5-thio-D-glucose. *Experimental and Clinical Endocrinology and Diabetes* **103**:83-97.
 82. Wang, Z. and Gleichmann, H. 1998. GLUT2 in pancreatic islets: crucial target molecule in diabetes induced with multiple low doses of streptozotocin in mice. *Diabetes* **47**:50–56.
 83. Weiss, R.B. 1982. Streptozotocin: a review of its pharmacology, efficacy, and toxicity. *Cancer Treatment Reports* **66**:427–438.
 84. Yang, H. and Wright, J.R. Jr. 2002. Human beta cells are exceedingly resistant to streptozotocin in vivo. *Endocrinology* **143(7)**:2491-2495.
 85. Yotsumoto, T., Naitoh, T., Shikada, K. and Tanaka, S.

1997. Effects of specific antagonists of angiotensin II receptors and captopril on diabetic nephropathy in mice. *Japanian Journal of Pharmacology* **75**:59-64.
86. Zafar, M., Naqvi, S.N., Ahmed, M. and Kaimkhani, Z.A. 2009a. Altered kidney morphology and enzymes in streptozotocin-induced diabetic rats. *International Journal of Morphology* **27(3)**:783-790.
87. Zafar, M., Naqvi, S.N.H., Ahmed, M. and Kaimkhani, Z.A. 2009b. Altered liver morphology and enzymes in streptozotocin induced diabetic rats. *International Journal of Morphology* **27(3)**:719-725.